# Lab on a Chip

Accepted Manuscript

This is an *Accepted Manuscript*, which has been through the Royal Society of Chemistry peer review process and has been accepted for publication.

Accepted Manuscripts are published online shortly after acceptance, before technical editing, formatting and proof reading. Using this free service, authors can make their results available to the community, in citable form, before we publish the edited article. We will replace this *Accepted Manuscript* with the edited and formatted *Advance Article* as soon as it is available.

You can find more information about *Accepted Manuscripts* in the **Information for Authors**.

Please note that technical editing may introduce minor changes to the text and/or graphics, which may alter content. The journal's standard **Terms & Conditions** and the **Ethical guidelines** still apply. In no event shall the Royal Society of Chemistry be held responsible for any errors or omissions in this *Accepted Manuscript* or any consequences arising from the use of any information it contains.

We demonstrate that a single micron-sized fluorescent bacterial cell can serve as laser gain

medium of droplet-based optofluidic biolasers.
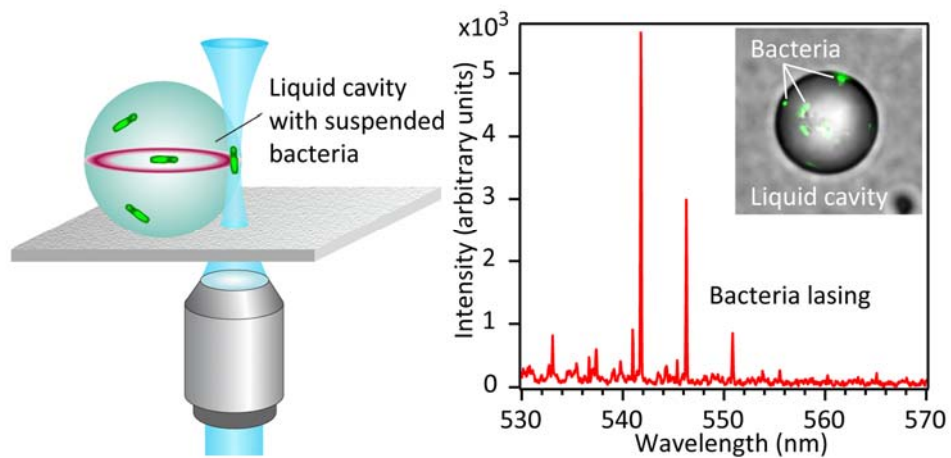
PAPER

In vitro and *in vivo* biolasing of fluorescent proteins suspended in liquid microdroplet cavities

Alexandr Jonáš,*[a] Mehdi Aas,[b] Yasin Karadag,[b] Selen Manioğlu,[c] Suman Anand,[d] David McGloin,[d] Halil Bayraktar,[c] and Alper Kiraz[b]

Fluorescent proteins are indispensable for selective, quantitative visualization of localization, dynamics, and interactions of key molecular constituents of live cells. Incorporation of fluorescent proteins into an optical cavity can lead to the significant increase of fluorescence signal levels due to stimulated emission [10] and light amplification in the cavity, forming a laser with biological gain medium. Utilization of lasing emission from fluorescent biological molecules can then greatly enhance the performance of fluorescence-based biosensors benefiting from the high sensitivity of non-linear lasing processes to small perturbations in the cavity and gain medium. Here we study optofluidic biolasers that exploit active liquid optical resonators formed by surface-supported aqueous microdroplets containing purified yellow [15] fluorescent protein or suspension of live *E. Coli* bacterial cells expressing the fluorescent protein. We first demonstrate lasing in fluorescent protein solutions at concentrations as low as 49 μM. Subsequently, we show that a single fluorescent bacterial cell of micrometre size confined in a droplet-based cavity can serve as laser gain medium. Aqueous droplet microcavities allow the maintenance of the bacterial cells at conditions compatible with unimpeded growth. Therefore, our results also suggest a direct route to [20] microscopic sources of laser light with self-regenerating gain media.

1. Introduction

Green fluorescent protein (GFP) and its engineered colour variants such as yellow fluorescent protein or cyan fluorescent protein are widely used experimental tools that have [25] revolutionized cell and molecular biology research [1]. The tremendous potential of fluorescent proteins in life sciences stems from the possibility of fusing them genetically to a number of important cellular components in both prokaryotic and eukaryotic organisms, without affecting the structure, function, or cellular [30] location of the fluorescently labelled target molecule [2]. Combined with advanced microscopy techniques such as Förster resonance energy transfer (FRET), fluorescent protein-based probes allow for understanding numerous biological phenomena at the molecular level, including highly selective and sensitive [35] quantitative detection of molecular components in complex environments (e.g., cell cytoplasm and membranes), visualization of protein expression and degradation in cells, and dynamics of molecular interactions [3].

In a typical live-cell experiment, the intensity of spontaneous [40] light emission from optically pumped fluorescent proteins expressed in cells is detected and evaluated. While this procedure is straightforward to implement, the level of the spontaneous fluorescence signal can be too low to collect a sufficiently high number of photons before the fluorophore photobleaches. [45] Amplified stimulated emission from fluorescent protein

molecules placed inside a suitable optical cavity can lead to lasing of the protein and, subsequently, the significant increase of the fluorescence intensity. Such biolasers can be used to implement new ways of biological sensing and analysis that [50] benefit from the high sensitivity of stimulated emission to small perturbations in the laser cavity and gain medium and from the specificity of attachment of fluorescent proteins to selected cellular components which allows targeted studies of well-defined intracellular processes [4].

[55] Biolasers can be readily integrated with existing optofluidic technologies; they can be combined with accurate control of fluids on small spatial scales and interfaced with optical waveguides or fibres in compact lab-on-a-chip systems. Gain media based on fluorescent proteins expressed in living cells can [60] be regenerated following photobleaching of the fluorophore; hence, biolasers are in principle self-healing. Furthermore, specific molecular recognition and self-assembly can provide additional functionality and programmatic control of photonic components based on biological molecules. The first [65] demonstrations of biolasing employed GFP-expressing live mammalian cells or *E. Coli* bacteria placed inside a Fabry-Perot resonator [5], [6]. Recently, an optofluidic ring resonator (OFRR) was used for observation of *in vitro* lasing from aqueous solutions of fluorescent proteins. This scheme was based on indirect pumping [70] of lasing emission via FRET and employed genetically encoded fluorescent protein pairs linked by a peptide with adjustable length, thus allowing studying protein-protein or protein-drug

interactions [7]. Biological molecules other than fluorescent proteins have also been recently tested as laser gain media. In these demonstrations, lasing was achieved with luciferin solution contained within an OFRR [8] or flavin mononucleotide dissolved in glycerol-water microdroplets supported by a superhydrophobic surface [9]. However, unlike fluorescent proteins, these small fluorescent organic compounds cannot be readily expressed and regenerated in living cells and selectively fused to other cellular proteins without external coupling agents.

In this article, we introduce optofluidic droplet-based biolasers with the gain medium effectively formed by an individual micron-sized bacterial cell suspended in the droplet liquid. The glycerol-water microdroplets supported by a superhydrophobic surface serve as optical cavities for the amplification of stimulated emission from the Venus variant of yellow fluorescent protein expressed in the bacteria. Liquid optical resonators based on surface-supported aqueous microdroplets combine key advantages of OFRRs and Fabry-Perot resonators. While the optical modes of Fabry-Perot resonator occupy relatively large mode volumes, OFRRs and spherical microdroplets host whispering gallery modes (WGMs) with very small mode volumes and high quality factors (Q-factors) [10]. These morphology-dependent optical resonances circulate in a narrow region near the internal surface of the cavity due to total internal reflection of light. As a result, very large optical intensities can be stored in WGMs. In an OFRR, however, the gain medium lies outside the cavity formed by the wall of a glass capillary tube and, thus, the gain medium only couples to the evanescent field of the WGMs circulating in the capillary wall. Hence, only the molecules within a narrow zone in the proximity of the capillary wall (less than 100 nm) can undergo stimulated emission, which makes lasing from fluorescent proteins expressed in live cells very difficult. In contrast, in both Fabry-Perot cavities and microdroplet resonators, optical modes circulate directly in the volume where the gain medium is located which implies strong interaction between the light and the gain medium. The above combination of characteristic features renders microdroplet-based resonators very suitable for non-linear optical studies such as biolasing using low optical pump intensities. In addition, aqueous microdroplets provide natural environmental conditions for biological molecules and live cells. In our experiments, we characterize lasing from surface-supported droplets containing either solutions of purified Venus fluorescent protein or dilute suspensions of *E. Coli* bacterial cells stably expressing the Venus protein. We study the dynamics of lasing from these laser gain media and provide experimental evidence for lasing from a single Venus-expressing bacterial cell.

2. Materials and Methods

2.1. Expression, isolation, and purification of Venus yellow fluorescent protein

All reagents were obtained from VWR International GmbH (Darmstadt, Germany) and used as received unless otherwise specified. In order to express Venus in BL21 *E. coli* cells, the Venus gene was cloned into the pBTR (Amp[r]) expression vector using standard cloning methods and the plasmid was subsequently inserted into the bacteria. After transformation,

BL21 cells were cultivated in 1L of LB-type growth medium for 1 hour at 37 °C. Grown cells were harvested from the medium by centrifugation for 10 minutes at 4.500 rpm and then resuspended in 50 mM phosphate buffer at pH 7. Cells in buffered suspensions were homogenized with a probe-tip sonicator. The resulting cell lysate was then ultra-centrifuged at 20.000 rpm for 15 minutes and the supernatant was collected and used in all lasing experiments. The emission and excitation fluorescence spectra of 5 μM Venus solution in 50 mM phosphate buffer were measured at 25 °C by FluoroMax-3 spectrofluorometer. The absorption spectra of suspended Venus-expressing BL21 cells were collected by Shimadzu UV-3600 spectrophotometer. For quantitative analysis of fluorescence intensity from purified Venus solutions and Venus-expressing *E. coli* cells, samples were imaged with an EMCCD camera (LucaS; Andor) operated in frame-transfer mode at 5 frames per second. Fluorescence emission data were analysed with ImageJ (NIH) and MATLAB (MathWorks) software packages.

2.2. Generation of liquid microdroplets supported by superhydrophobic surfaces

Superhydrophobic surfaces with water contact angles > 150° for droplet deposition were prepared by spin coating hydrophobic silica nanoparticles (Aeroxide LE2; Evonik) dispersed in ethanol on cleaned coverslips [11]. To deposit micron-sized droplets on the surface, liquid aerosols containing the laser gain medium in the form of either purified Venus protein or fluorescent bacteria in a mixture of water and glycerol were generated using a compact ultrasonic nebulizer (JIH50, Beuer) and sprayed over the surface. This procedure provided surface-supported microdroplets with radii ranging from 0.5 μm to 50 μm; in case of bacterial suspensions, the mixture was diluted until the droplets contained approximately 5 – 15 bacteria per droplet with ~5 μm radius. The number of bacteria in the selected droplet was estimated by direct counting of the suspended cells. In order to obtain in-focus image of the cells, the position of the microscope focal plane within the droplet was gradually adjusted during counting.

2.3. Fluorescence spectroscopy of lasing microdroplets

A detailed scheme of the inverted optical microscope system used for recording emission spectra from surface-supported fluorescent microdroplets is shown in ESI† Fig. S1. An individual selected droplet resting on the superhydrophobic surface was optically pumped with a pulsed femtosecond 488 nm laser beam (pulse width 140 fs, repetition rate 80 MHz - Chameleon Ultra II; Coherent) in 5 μs bunches of pump pulses (approximately 400 pulses per bunch – see ESI† Fig. S2). In order to minimize the distortion of the studied droplet shape by intense laser pulses, a single bunch of excitation pulses was used for recording an emission spectrum of the droplet. The excitation beam was focused at the rim of the studied droplet using a high NA water-immersion microscope objective lens (60x, NA = 1.2; Nikon) to a diffraction-limited spot with the radius of approximately 0.4 μm. Fluorescence emission from the droplets was then collected using the same microscope objective and analysed with an imaging spectrometer.
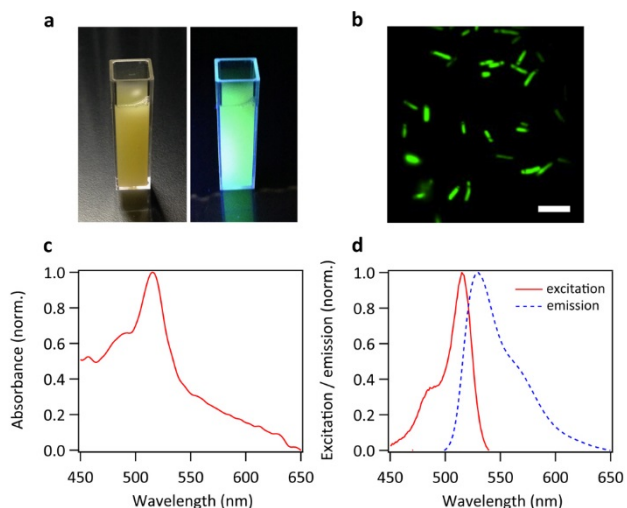
Fig. 1 Venus-expressing *E. coli* cells as the laser gain medium.

a, Image of aqueous suspension of BL21-strain of *E. coli* bacterial cells
expressing Venus variant of the yellow fluorescent protein under white
light illumination (left) and UV light illumination (right). **b,** Pseudocolor
fluorescence image of BL21 cells expressing Venus fluorescent protein.
Scale bar is 5 μm. **c,** Absorption spectrum of aqueous suspension of BL21
cells expressing Venus fluorescent protein. **d,** Excitation and emission
spectra of purified Venus fluorescent protein suspended in 50 mM
phosphate buffer.

3. Results

3.1. Characterization of Venus fluorescent protein and Venus-expressing bacterial cells

Venus yellow fluorescent protein has been frequently used as a reporter for the quantification of protein expression levels [12], [13], [14], [15], [16]. Since Venus has a high quantum yield of $\Phi = 0.57$ [17] and it is one of the brightest fluorophores among all fluorescent proteins [18], it is an excellent candidate for the gain medium of optofluidic biolasers. In our experiments, Venus was expressed in BL21 *E. coli* cells using pBTR high-expression vector. The resulting high intracellular concentration of the fluorophore is a prerequisite for observation of live-cell lasing emission with a low pump laser power. In Fig. 1a, an aqueous suspension of Venus-expressing BL21 bacterial cells is shown under white light illumination (left) and UV light illumination (right). In both imaging modes, the bacterial suspension displays intense colour (yellow for the transmitted white light image, light green for the fluorescence image) indicative of a high Venus expression level in BL21 cells. Individual fluorescent bacteria deposited on a cover slip surface could be clearly imaged after wide-field illumination with 473 nm laser light (Fig 1b). To determine the maximum absorption wavelength of Venus under *in vivo* conditions, we acquired the visible absorption spectrum of an aqueous suspension of fluorescent BL21 cells at pH 7.0 (Fig. 1c). In this spectrum, the main absorption peak of intracellular Venus at 515 nm is superimposed on the monotonically decreasing spectral background caused by light scattering from the cells. The spectrum also features a secondary absorption shoulder around 488 nm, which was used in the Venus lasing experiments. Further information about the spectral properties of Venus was obtained

from the fluorescence excitation and emission spectra of the solutions of purified Venus in 50 mM phosphate buffer (Fig. 1d). The concentration of Venus in the buffer solution (5 μM) was determined from its recorded visible absorption spectrum and known molar extinction coefficient [12]. The spectral peak of Venus fluorescence emission recorded with 470 nm excitation light was observed to lie at 530 nm. Identical to the live-cell absorption spectrum of Fig. 1c, the fluorescence excitation spectrum displays a maximum at 515 nm. This suggests that the high expression level of Venus in the bacteria does not have a significant influence on the spectral characteristics and the fluorescence brightness of the protein. In order to estimate the concentration of Venus in living BL21 cells, we compared the intensity of fluorescence from individual cells and Venus solution of a known protein concentration (see ESI† text and Fig. S3). The average intracellular concentration of Venus c_B was found to be approximately 470 μM. Considering a typical *E. coli* cell volume V_B of $0.20 - 0.77$ fl (cell approximated by a cylinder with the diameter of 0.5-0.7 μm and length of 1-2 μm), this corresponds to about $N_A V_B c_B \approx 60,000 - 220,000$ copies of Venus per cell (N_A is Avogadro's number).

3.2. Observation of lasing from aqueous solutions of Venus fluorescent protein

Liquid microdroplets supported by superhydrophobic (SH) surfaces have been successfully used as optical resonant cavities in the studies of lasing from aqueous solutions of fluorescent dyes [11] and vitamins [9]. Deposition of droplets on an SH surface with a high liquid-solid contact angle preserves the spherical shape of the droplets and stabilizes their position. Moreover, with transparent droplet-supporting substrates, light can be easily coupled into and out of the droplets using an inverted optical microscope (Fig. 2a). In our experiments, we obtained transparent SH surfaces by spin-coating a solution of hydrophobic silica nanoparticles on clean glass coverslips. The studies of lasing from aqueous solutions of Venus fluorescent protein were carried out using Venus dissolved in 35% v/v mixture of glycerol and 50 mM phosphate buffer. Presence of low-volatility glycerol in the droplet liquid is essential for stabilizing the droplets exposed to ambient room atmosphere against evaporation [19]. Under typical experimental conditions (temperature 26 °C, relative humidity 64%), the final equilibrium concentration of glycerol in the phosphate buffer solution was estimated to be approximately 64% v/v; this corresponds to the reduction of the droplet volume by a factor of 0.55 and, consequently, the increase of the Venus concentration in the droplets with a factor of 1.81. All concentrations of Venus in droplets reported in this article are the final values that take into account partial liquid evaporation after the droplet generation. Venus-containing liquid droplets were deposited on the SH surface using a compact ultrasonic nebulizer. Subsequently, fluorescence from individual droplets was excited by focusing a femtosecond (fs) pulsed laser beam with the wavelength of 488 nm at the droplet rim using a microscope objective of a high numerical aperture. Light emitted from the droplet was collected by the same objective lens and analysed by a spectrograph (see ESI† text and Fig. S1 for details).

In Figs. 2b – 2d, emission spectra are presented which were recorded from a single surface-supported droplet with Venus
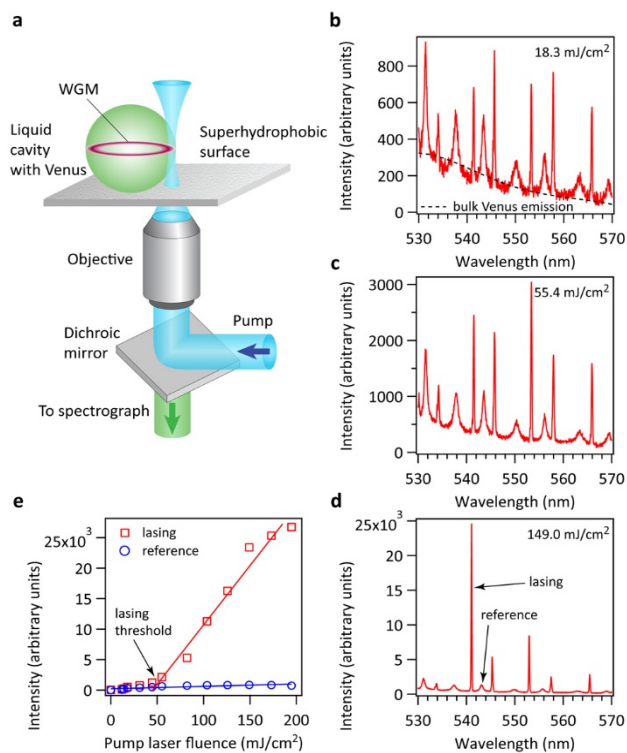
Fig. 2 Lasing of Venus fluorescent protein in surface-supported microdroplets.

a, Experimental geometry for observation of lasing from the solution of purified Venus fluorescent protein contained in a surface-supported glycerol-water microdroplet acting as a liquid optical resonant cavity. Figure is not drawn to scale. **b**, Example of droplet emission spectrum recorded with a pump beam fluence below the lasing threshold. Black dashed line shows the bulk emission spectrum of Venus fluorescent protein solution (no cavity modes). **c**, Example of droplet emission spectrum recorded with a pump beam fluence near the lasing threshold. **d**, Example of droplet emission spectrum recorded with a pump beam fluence above the lasing threshold. **e**, Intensity of the lasing and reference spectral peaks indicated in part **d** as a function of the pump laser fluence. Symbols denote experimental data, solid lines denote linear fits to the data. Droplet radius is 3.2 μm.

concentration of 49 μM and consecutively increasing fluence of the pump laser beam. At the lowest excitation fluence of 18.3 mJ/cm^2 (Fig. 2b), the pump energy is not sufficient to achieve lasing for the given Venus concentration. The resulting droplet emission spectrum features a number of non-amplified WGMs of comparable intensity and varying width superimposed on a broad non-resonant background of bulk Venus fluorescence. The observed WGMs correspond to different resonant paths of the light in the droplet and can be uniquely identified by their radial, angular, and azimuthal mode numbers and mode polarization (TE or TM) [20]. In general, WGMs with the lowest radial mode number $n = 1$ that circulate closest to the droplet surface display the highest Q-factors and, thus, they are the best candidates for the observation of lasing [21]. When the pump fluence goes up to 55.4 mJ/cm^2, the intensity of these narrowest WGMs increases by a larger factor than the intensity of broad WGMs and non-resonant spectral background (Fig. 2c). Stronger dependence of the intensity of high-Q WGMs on the pump fluence indicates the onset of nonlinear optical phenomena associated with amplified

stimulated emission from the droplets. With the pump fluence set to 149 mJ/cm^2, well above the lasing threshold of the studied droplet, the intensity of lasing WGMs relative to non-lasing optical modes and non-resonant background increases dramatically (Fig. 2d). The spectral location of the overall maximum of lasing emission is then determined by the interplay between the Venus absorption and emission profiles, Venus concentration in the droplet, and droplet size. Generally, the strongest lasing peak is shifted to the red from the bulk emission maximum of the fluorophore due to the self-absorption that increases absorptive losses of the cavity at shorter emission wavelengths [22].

In order to quantify the pump threshold required for droplet lasing, we recorded and analysed a series of droplet emission spectra with gradually increasing fluence of the pump beam. In Fig. 2e, the intensity above background for lasing and reference WGMs annotated in Fig. 2d is plotted as a function of the pump fluence. From this figure, it is obvious that upon exceeding a certain pump level, intensities of the lasing and reference WGMs start growing with a different rate, which marks the onset of lasing. The actual threshold value of 44.5 mJ/cm^2 was determined from the intersection of line fits to the experimental data points obtained for the reference WGM (over the whole range of studied pump fluences) and lasing WGM (pump fluences above 46 mJ/cm^2). After crossing the threshold, full width at half maximum (FWHM) of the reference WGM remains more less constant (~0.65 nm) whereas FWHM of the lasing WGM decreases by approximately 20% from 0.22 nm to 0.18 nm (see ESI† Fig. S4) due to the nonlinear interactions between the amplified resonant light and molecules of the gain medium [11]. Similar to regular fluorescent dyes, the pump threshold of Venus-based microdroplet lasers is a function of the protein concentration in the droplets and droplet radius, as both of these factors influence the overall losses of the cavity [22].

3.3. Stability of lasing from aqueous Venus solutions

Since the total amount of Venus fluorescent protein contained in any given droplet is constant, the effective lifetime of droplet-based microlasers using Venus as the gain medium is limited by the rate of protein photobleaching. In order to characterize the Venus photobleaching dynamics, we recorded time series of lasing spectra from individual Venus-containing droplets using a constant fluence of the pump beam. Figure 3a displays a typical series of emission spectra acquired from a 2.4 μm radius droplet containing 49 μM Venus solution. The effective acquisition time for each spectrum was ~5 μs, corresponding to the duration of the bunch of excitation pulses (see ESI† Fig. S2), and the delay between individual spectral frames was 1 s. Constant excitation fluence of 246 mJ/cm^2 was set to be above the initial lasing threshold that characterizes the droplets before any Venus photobleaching has taken place. In Fig. 3a, WGM at 533 nm labelled "lasing" is amplified via stimulated emission within the droplet cavity whereas WGM at 539 nm labelled "reference" represents regular spontaneous emission. These two WGMs belong to different mode families with identical radial mode numbers and different polarizations: TM for the lasing WGM and TE for the reference WGM [23]. The lasing WGM has a smaller initial FWHM than the reference WGM (0.26 nm vs. 0.37 nm)
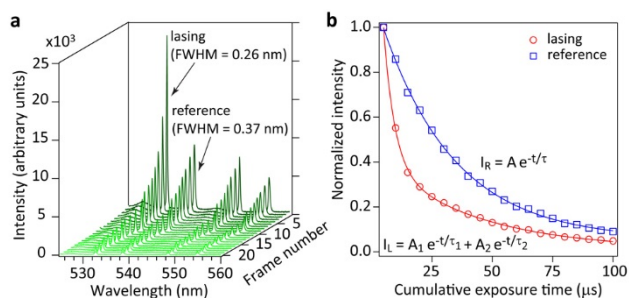
Fig. 3 Stability of lasing from Venus protein solutions.

a, Time series of the lasing emission spectra recorded with a constant
pump fluence from a surface-supported microdroplet with the radius of
2.4 μm. **b**, Time evolution of the normalized intensity of lasing and
reference WGMs denoted in part **a**. Symbols indicate experimental data
points, solid lines indicate double-exponential (lasing WGM intensity I_L)
or single-exponential (reference WGM intensity I_R) fits of the
experimental data.

which translates into higher Q-factor of the lasing WGM. From
Fig. 3a, it is obvious that the intensity of all WGMs in the
spectrum monotonically decreases with growing acquisition
frame number due to increasing total exposure of the droplet to
the pump beam and, consequently, higher Venus photobleaching.

More quantitative insight into the photobleaching processes
can be obtained from the analysis of the time evolution of the
WGM intensity presented in Fig. 3b. In this figure, normalized
amplitudes above the spectral background of the lasing and
reference WGMs are plotted as a function of the cumulative
exposure time of the droplet to the pump beam. Here, amplitudes
of both modes are normalized to their respective initial values in
the first recorded spectral frame. Comparison of the experimental
data recorded for the lasing and reference WGMs reveals
different dynamics of intensity decay of both modes. While the
intensity I_R of the reference WGM decreases with a single-
exponential decay of the form $I_R = A \exp(-t/\tau)$, the intensity I_L of
the lasing WGM cannot be described using a single-exponential
decay, following instead a double-exponential decay $I_L = A_1 \exp(-t/\tau_1) + A_2 \exp(-t/\tau_2)$; adding further exponential terms does not
lead to a significant change of the fit residuals. The intensity of
the remaining two WGMs and spectral background falls off
exponentially with the same characteristic time as the reference
WGM. In homogeneous aqueous solutions of fluorescent
molecules, the photobleaching reaction can be regarded as being
quasi-unimolecular and, thus, fluorophore concentration
decreases exponentially with time [24]. This notion agrees with the
observed behaviour of the intensity of non-lasing WGMs and
non-resonant spectral background originating from spontaneous
emission which depends linearly on the Venus concentration. On
the other hand, Venus lasing involves non-linear optical
processes that underlie amplified stimulated emission taking
place in the droplet-based optical resonator. Overall cavity gain
and losses depend on the actual Venus concentration in the cavity
and their interplay determines the pump threshold and the
intensity of the lasing peak. As the fluorescent protein
progressively bleaches, pump threshold required for lasing
gradually increases until it exceeds the actual used pump fluence;
at this point, lasing action ceases. A double-exponential fit to the
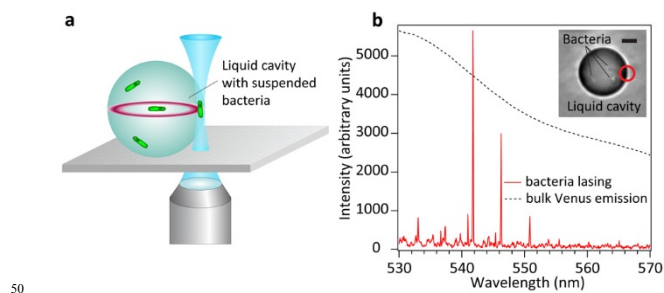
**Fig. 4 Lasing of fluorescent *E. coli* bacterial cells in surface-supported
microdroplets.**

a, Experimental geometry for observation of lasing from live *E. coli*
bacterial cells expressing Venus fluorescent protein. The bacteria are
suspended and freely mobile in glycerol-water microdroplets standing on
a superhydrophobic surface. The figure is not drawn to scale. **b**, Example
of lasing emission spectrum recorded from suspended *E. coli* bacterial
cells (solid line). For comparison, emission spectrum of purified bulk
solution of Venus fluorescent protein is also shown (dashed black line).
Inset is the image of the actual droplet (radius 8.4 μm) used for spectral
recording that contains ~7 bacterial cells. Circle indicates location of the
excitation beam spot on the droplet. The scale bar is 5 μm.

temporal profile of the lasing WGM intensity shown in Fig. 3b
gives two characteristic decay times $\tau_1 = 4.5$ μs and $\tau_2 = 40.5$ μs.
On the fast time scale described by τ_1, WGM emission is
dominated by lasing that eventually changes to spontaneous
emission when the slow time scale τ_2 is reached. This
interpretation is supported by the measured characteristic decay
time τ of the reference WGM that is found to be $\tau = 30$ μs,
comparable to τ_2. Gradual decrease of the lasing contribution to
the overall emission intensity is also accompanied by broadening
of the lasing WGM whose FWHM increases to 0.36 nm after
cumulative exposure of 100 μs and, thus, becomes comparable to
the FWHM of the reference WGM (see ESI† Fig. S5).

The lifetime of the first excited electronic state of Venus
fluorescent protein from which stimulated emission to the ground
electronic state occurs is approximately 3 ns [25]. The femtosecond
pump laser used in our experiments has pulse repetition rate of 80
MHz, which corresponds to pulse-to-pulse separation of 12.5 ns,
longer than the fluorescence lifetime. Thus, lasing emission from
the droplets can be excited with a single pump pulse. A typical
spectral frame shown in Fig. 3a is acquired with ~400 pump
pulses. Assuming 100 % efficiency of the pumping, ~400 lasing
pulses are emitted from the droplet in a single spectrum. Since
lasing is typically observable in several consecutive spectral
frames before Venus bleaches, minimal useful output of droplet-
based microlasers is a few thousands pulses.

3.4. Observation of lasing in suspensions of bacteria expressing Venus fluorescent protein

After characterizing basic properties of droplet-based microlasers
with aqueous solutions of purified Venus fluorescent protein, we
carried out experiments in which the laser gain medium was
formed by dilute suspensions of living BL21 *E. coli* bacteria
stably expressing Venus. To this end, bacterial cells were
suspended in 35% v/v mixture of glycerol and 50 mM phosphate

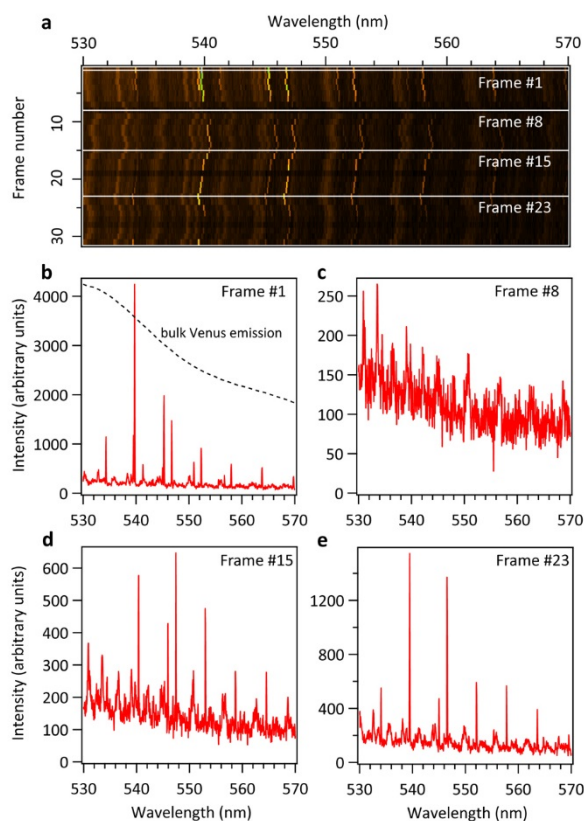**Fig. 5 Dynamics of lasing from suspended *E. coli* bacterial cells.**

a, Time series of emission spectra recorded from a bacteria-containing
droplet of 6.8 μm radius with a constant pump fluence. The number of
bacterial cells in the droplet was ~10. **b-e,** Droplet emission spectra for
frames 1, 8, 15, and 23 indicated by white horizontal lines in part **a**. Due
to bacteria diffusion and active motion into and out of the excitation
volume, droplet emission pattern in different frames switches between
lasing and non-lasing emission mode.

buffer (initial glycerol concentration prior droplet generation and
partial evaporation – see the discussion in section 3.2.
"Observation of lasing from aqueous solutions of Venus
fluorescent protein"). Subsequently, liquid droplets were
deposited on SH surface using a nebulizer. Cell concentration in
the suspension was adjusted so as to obtain approximately 5 – 15
bacteria per droplet with ~5 μm radius. In order to excite
fluorescence in the droplets, the pump laser beam was focused at
the droplet rim over a suitably positioned bacterial cell (see Fig.
4a and inset of Fig. 4b for details of the excitation geometry).
Figure 4b shows an example emission spectrum recorded from an
8.4 μm radius droplet containing ~7 bacterial cells. The excitation
fluence used for recording the spectrum was 312 mJ/cm² and the
effective acquisition time was 5 μs. Sharp lasing WGMs observed
between 540 – 555 nm are shifted to the red with respect to the
emission maximum of bulk Venus solution (530 nm) due to self-
absorption induced losses at shorter emission wavelengths.
FWHM of lasing WGMs in the bacterial suspension (0.13 nm) is
comparable to FWHM of the lasing peak in Venus solution (0.18
nm – see Fig. 2d) which implies comparable Q-factors and,
consequently, negligible distortion of the droplet shape and
minimal scattering losses due to the presence of bacteria in the

liquid.

Unlike in the case of droplets containing purified Venus
solution, laser gain medium represented by individual fluorescent
bacterial cells is discrete, with random and non-uniform
distribution within the liquid cavity. Moreover, the cells can
move freely in the liquid due to diffusion and active motion. The
size of the effective excitation volume formed in the vicinity of
the pump beam focus is comparable to the wavelength of the
pump beam and, thus, only a single bacterial cell typically resides
within this high-intensity excitation region. Additional restriction
on the permissible location of the lasing bacterium within the
droplet arises from the requirement of a sufficient overlap of the
bacterium with the WGM modal volume, which is a prerequisite
for the observation of stimulated emission. As argued in Section
3.2, lasing is associated with the highest-Q WGMs characterized
by the lowest radial mode number $n = 1$ [21]. These WGMs are
confined to radial distances r from the droplet centre of $0.9a < r <
a$ where a is the droplet radius [26]. For the typical size of droplets
used in our lasing experiments ($a < 10$ μm), the thickness of the
spherical shell near the droplet surface within which the
stimulated emission can take place lies in the sub-micron range.
The limited spatial extent of the excitation region and the modal
volume of WGMs together with the random motion of the
bacteria into and out of the excitation volume lead to distinctive
on-off character of the lasing emission from dilute bacterial
suspensions contained in the droplets. Figure 5a presents time
series of fluorescence emission spectra recorded from a droplet
with 6.8 μm radius containing approximately 10 bacterial cells. A
constant pump fluence of 312 mJ/cm² was used, with an effective
integration time for acquiring each spectrum in the series of 5 μs,
and a total of 32 spectra were recorded with a time delay of 1 s
between successive spectra. In the 2-D spectrum of Fig. 5a,
random frame-to-frame intensity fluctuations are clearly
observable. In addition, small variations in the spectral positions
of individual WGMs appear which may be attributed to changes
in the WGM resonant path length induced by random diffusion of
the cells through the mode path and fluctuations of the droplet
cavity size caused by interplay between the droplet evaporation
and condensation during optical pumping [19]. Four selected
spectral frames highlighted by white horizontal lines in Fig. 5a
and shown in detail in Figs. 5b – 5e illustrate the dynamics of the
droplet emission pattern. From initial lasing in frame #1, droplet
emission progresses to an almost dark state with very low
emission intensity in frame #8, as the bacterium forming the laser
gain medium tumbles in the liquid (see ESI† Video1 and Video2
for illustration of bacterial motion). Subsequently, the bacterium
approaches the excitation volume again, displaying regular non-
amplified WGMs in frame #15, and the droplet then returns back
to lasing in frame #23. During the random motion of the selected
bacterium through the excitation volume, transitions from
amplified stimulated emission to spontaneous emission are
marked by large fluctuations of the WGM intensity. Moreover,
frame-to-frame changes of the cell position and orientation also
result in changes of the relative intensity of individual lasing
WGMs since their relative gain and losses are highly sensitive to
small perturbations in the liquid cavity.

4. Discussion

We have demonstrated and characterized lasing from active liquid optical microcavities formed by surface-supported water/glycerol microdroplets containing purified Venus fluorescent protein or dilute suspension of live *E. coli* bacterial cells expressing stably the Venus protein. Using aqueous Venus solutions, we have shown that lasing can be achieved with Venus concentration in the droplet as low as a few tens of μM, which compares favourably to microdroplet lasers that exploit traditional organic dyes [11]. With femtosecond pulsed laser excitation, optofluidic biolasers based on Venus-containing microdroplets can emit several thousand pulses before the fluorophore photobleaches. As suggested by Eggeling *et al.*, detrimental effects of photobleaching on the useful operation time of such droplet-based microlasers can be moderated by using excitation wavelengths closer to the Venus absorption maximum (515 nm) and longer excitation pulses [27]. Alternatively, Venus can be replaced with a different fluorescent protein that displays a better photostability [17]. Our studies of lasing in microdroplets prepared from dilute aqueous suspensions of fluorescent *E. coli* bacteria expressing Venus have provided experimental evidence for the feasibility of such biolasers with active gain medium formed by live cells suspended in a liquid, under environmental conditions compatible with cell survival. Distinctive on-off character of lasing emission from bacterial suspensions supports the notion of single fluorescent bacterium being sufficient as the laser gain medium. Irradiation of the selected bacterial cell serving as the laser gain medium with the high-fluence pump beam raises the question of viability of the cell upon prolonged light exposure. Even though we did not observe any obvious changes in the integrity of the irradiated cells after recording the spectra, we cannot rule out a more subtle damage of vital organelles of the cell. Daddysman and Fecko studied localized damage of DNA in eukaryotic cells induced by multi-photon absorption of focused fs laser pulses with the pulse width, repetition rate, wavelength, and focal spot radius very similar to our experiments [28]. They found out that the total energy of 100 – 300 nJ deposited to the specimen (He-La cells or polytene nuclei of *Drosophila* salivary gland cells) is sufficient to cause observable DNA damage. In our experiments with bacteria lasing, the typical energy deposited to the lasing cell for recording a single spectral frame was approximately 600 nJ (120 mW of mean power at the specimen with 5 μs exposure time). Thus, it is quite likely that the bacterial DNA was at least partially damaged. However, in our case, not all of the pump laser energy reaching the specimen was actually absorbed by the DNA. In *E. coli*, nucleoid (the bacterial chromosome) typically occupies a region with the volume of about 0.23 μm^3 which corresponds to a sphere with the radius of approximately 0.38 μm [29], equal to the radius of the pump beam waist used in our study (~0.40 μm). Since the Venus-expressing irradiated cells displayed strong fluorescence, it follows that a significant part of the pump light was absorbed by the fluorescent protein and, thus, it did not reach the DNA. Moreover, even if the originally selected lasing cell is irreversibly damaged by the pump beam, other cells within the same droplet that have not been exposed to the pump light are unaffected and, consequently, they can be used as the gain medium in the next trial.

5. Conclusion

We introduced and systematically studied miniature optofluidic biolasers based on surface-supported liquid microdroplet cavities containing either purified yellow fluorescent protein or live *E. coli* bacteria expressing this protein. Initially, we demonstrated that micromolar protein concentrations in aqueous microdroplets are sufficient for sustained lasing. Subsequently, we showed that a single micron-sized fluorescent bacterial cell can serve as living laser gain medium. The lasing bacteria suspended in a droplet can be provided with all nutrients required for steady growth, which may allow for extending the operation time of this biologically controlled source of laser light by active regeneration of the gain medium. Using bacterial strains expressing two different fluorescent proteins that form a FRET donor-acceptor pair, non-radiative energy-transfer mechanism can be used for laser pumping which would further improve lasing efficiency and open up the possibility for emission wavelength tuning [30]. Furthermore, FRET lasing in connection with self-recognition and self-assembly of biological molecules attached to the fluorescent proteins can be exploited to program and modulate the laser characteristics, thus paving the way to new routes of live-cell bio-sensing.

Notes and references

^{a} *Department of Physics, Istanbul Technical University, Maslak 34469, Istanbul, Turkey. E-mail: ajonas@itu.edu.tr*
^{b} *Department of Physics, Koç University, Rumelifeneri Yolu, Sariyer 34450, Istanbul, Turkey. E-mail: akiraz@ku.edu.tr*
^{c} *Department of Chemistry, Koç University, Rumelifeneri Yolu, Sariyer 34450, Istanbul, Turkey.*
^{d}*School of Engineering, Physics and Mathematics, University of Dundee, Nethergate, Dundee DD1 4HN, United Kingdom.*
† Electronic Supplementary Information (ESI) available: See DOI: 10.1039/b000000x/

1. S. J. Remington, *Protein Sci.*, 2011, **20**, 1509-1519.
2. J. Wiedenmann, F. Oswald and G. U. Nienhaus, *Iubmb Life*, 2009, **61**, 1029-1042.
3. M. Zimmer, *Chem. Rev.*, 2002, **102**, 759-781.
4. X. Fan and S. H. Yun, *Nat. Methods*, 2014, **11**, 141-147.
5. M. C. Gather and S. H. Yun, *Nat. Photonics*, 2011, **5**, 406-410.
6. M. C. Gather and S. H. Yun, *Opt. Lett.*, 2011, **36**, 3299-3301.
7. Q. S. Chen, X. W. Zhang, Y. Z. Sun, M. Ritt, S. Sivaramakrishnan and X. D. Fan, *Lab. Chip*, 2013, **13**, 2679-2681.
8. X. Wu, Q. Chen, Y. Sun and X. Fan, *Appl. Phys. Lett.*, 2013, **102**, 203706.
9. S. Nizamoglu, M. C. Gather and S. H. Yun, *Adv. Mater.*, 2013, **25**, 5943-5947.
10. Y. Z. Sun and X. D. Fan, *Anal. Bioanal. Chem.*, 2011, **399**, 205-211.
11. A. Kiraz, A. Sennaroglu, S. Doganay, M. A. Dundar, A. Kurt, H. Kalaycioglu and A. L. Demirel, *Opt. Commun.*, 2007, **276**, 145-148.

12. T. Nagai, K. Ibata, E. S. Park, M. Kubota, K. Mikoshiba and A. Miyawaki, *Nat. Biotechnol.*, 2002, **20**, 87-90.
13. T. Nagai, S. Yamada, T. Tominaga, M. Ichikawa and A. Miyawaki, *P. Natl. Acad. Sci. USA*, 2004, **101**, 10554-10559.
14. J. Yu, J. Xiao, X. J. Ren, K. Q. Lao and X. S. Xie, *Science*, 2006, **311**, 1600-1603.
15. M. Drobizhev, N. S. Makarov, S. E. Tillo, T. E. Hughes and A. Rebane, *Nat. Methods*, 2011, **8**, 393-399.
16. A. Miyawaki, *Annu. Rev. Biochem.*, 2011, **80**, 357-373.
17. N. C. Shaner, P. A. Steinbach and R. Y. Tsien, *Nat. Methods*, 2005, **2**, 905-909.
18. G. J. Kremers, S. G. Gilbert, P. J. Cranfill, M. W. Davidson and D. W. Piston, *J. Cell. Sci.*, 2011, **124**, 157-160.
19. A. Kiraz, Y. Karadag and M. Muradoglu, *Phys. Chem. Chem. Phys.*, 2008, **10**, 6446-6454.
20. G. C. Righini, Y. Dumeige, P. Feron, M. Ferrari, G. N. Conti, D. Ristic and S. Soria, *Riv. Nuovo Cimento*, 2011, **34**, 435-488.
21. J. D. Eversole, H. B. Lin and A. J. Campillo, *Appl. Optics.*, 1992, **31**, 1982-1991.
22. M. Aas, A. Jonas and A. Kiraz, *Opt. Commun.*, 2013, **290**, 183-187.
23. V. D. Ta, R. Chen and H. D. Sun, *Sci Rep-Uk*, 2013, **3**.
24. C. Eggeling, J. Widengren, R. Rigler and C. A. M. Seidel, *Anal. Chem.*, 1998, **70**, 2651-2659.
25. P. Sarkar, S. V. Koushik, S. S. Vogel, I. Gryczynski and Z. Gryczynski, *J. Biomed. Opt.*, 2009, **14**.
26. J. D. Eversole, H. B. Lin, C. D. Merritt and A. J. Campillo, *Appl. Spectrosc.*, 1994, **48**, 373 - 381.
27. C. Eggeling, A. Volkmer and C. A. M. Seidel, *Chemphyschem*, 2005, **6**, 791-804.
28. M. K. Daddysman and C. J. Fecko, *Biophys. J.*, 2011, **101**, 2294-2303.
29. C. L. Woldringh and N. Nanninga, *J. Struct. Biol.*, 2006, **156**, 273-283.
30. E. Özelci, M. Aas, A. Jonáš and A. Kiraz, *Laser Phys. Lett.*, 2014, **11**, 045802.